1

This preprint is the final accepted version of the article published in
Journal of Phycology, Volume 56, Issue 3, June 2020 Pages 818-829
https://doi.org/10.1111/jpy.12983

EFFECTS OF TEMPERATURE AND NUTRIENT SUPPLY ON RESOURCE ALLOCATION, PHOTOSYNTHETIC STRATEGY AND METABOLIC RATES OF *SYNECHOCOCCUS* SP.[1]

Cristina Fernández-González[2], Department of Ecology and Animal Biology, Universidade de Vigo, 36310 Vigo, Spain.

María Pérez-Lorenzo, Department of Ecology and Animal Biology, Universidade de Vigo, 36310 Vigo, Spain.

Nicola Pratt, School of Ocean and Earth Science, University of Southampton, SO14 3ZH Southampton, UK.

C. Mark Moore, School of Ocean and Earth Science, University of Southampton, SO14 3ZH Southampton, UK.

Thomas S. Bibby, School of Ocean and Earth Science, University of Southampton, SO14 3ZH Southampton, UK.

Emilio Marañón, Department of Ecology and Animal Biology, Universidade de Vigo, 36310 Vigo, Spain.

[2]Author for correspondence:

Cristina Fernández-González

Tel: +34 986818790

E-mail: c.fernandez@uvigo.es

Abstract

Temperature and nutrient supply are key factors that control phytoplankton ecophysiology, but their role is commonly investigated in isolation. Their combined effect on resource allocation, photosynthetic strategy and metabolism remain poorly understood. To characterize the photosynthetic strategy and resource allocation under different conditions, we analysed the responses of a marine cyanobacterium (*Synechococcus* PCC 7002) to multiple combinations of temperature and nutrient supply. We measured the abundance of proteins involved in the dark (RuBisCO, RbcL) and light (Photosystem II, PsbA) photosynthetic reactions, the content of chlorophyll *a*, carbon and nitrogen, and the rates of photosynthesis, respiration, and growth. We found that RbcL and PsbA abundance increased with nutrient supply, whereas a temperature-induced increase in PsbA occurred only in nutrient-replete treatments. Low temperature and abundant nutrients caused increased RuBisCO abundance, a pattern we observed also in natural phytoplankton assemblages across a wide latitudinal range. Growth, photosynthesis and respiration increased with temperature only under nutrient-sufficient conditions. These results suggest that nutrient supply exerts a stronger effect than temperature upon both photosynthetic protein abundance and metabolic rates in *Synechococcus* sp. and that the temperature effect on photosynthetic physiology and metabolism is nutrient dependent. The preferential resource allocation into the light instead of the dark reactions of photosynthesis as temperature rises is likely related to the different temperature dependence of dark-reaction enzymatic rates versus photochemistry. These findings contribute to our understanding of the strategies for photosynthetic energy allocation in phytoplankton inhabiting contrasting environments.

Keywords: Activation energy, D1 (PsbA) protein of PSII, Metabolic rates, Photosynthetic

strategy, RuBisCO, Temperature, Nutrient supply.

List of abbreviations: N-limited, nutrient limited, N-replete, nutrient replete, E_a, activation energy, P^C, Carbon-specific photosynthesis, P^{Chla}, Chlorophyll *a*-specific photosynthesis, R^C, Carbon-specific respiration, C:N, carbon to nitrogen ratio, C:Chl*a*, carbon to chlorophyll *a* ratio, POC, particulate organic carbon, PON, particulate organic nitrogen, μ_{max}, maximum growth rate.

Introduction

Rising sea surface temperatures, associated with increasing nutrient limitation in low-latitude, open-ocean regions, and growing anthropogenic eutrophication of the coastal zone represent some of the most pervasive effects of global change in marine ecosystems (Doney et al. 2012). Temperature and nutrient supply play key roles in controlling both resource allocation at the individual level and rates at which materials move through food webs, thus contributing to regulation of ecosystem functioning (Cross et al. 2015). Temperature influences phytoplankton directly through its effect on growth and metabolic rates (Eppley 1972, Chen et al. 2014). This effect is mostly related to kinetic responses such as increasing enzyme and ribosome activity as temperature rises (Geider 1987), which lead to enhanced rates of protein synthesis, light-saturated photosynthesis, and growth (Raven and Geider 1988). Equally important are nutrients, which are used to synthesize essential biomolecules, including the photosynthetic machinery, that sustain biochemical functions. The significance of nutrients lies in the fact that there is often a mismatch between their availability in the environment and the demands from organisms (Cross et al. 2015). Considering that as much as 80% of the global ocean is nutrient limited (Moore et al. 2013), an understanding of how phytoplankton acclimate and adapt to temperature must also consider the role of nutrient supply.

69 However, the effect of temperature upon phytoplankton metabolic rates and growth
70 has been studied mostly under nutrient-replete conditions. Only recently has the combined
71 effect of these two variables been investigated in the laboratory (Skau et al. 2017, Marañón
72 et al. 2018) and in the field (Lewandowska et al. 2014, Marañón et al. 2014, Morán et al.
73 2018). These studies suggest that the temperature effect may depend on nutrient
74 availability, such that metabolic rates may be more responsive to temperature when there is
75 a high nutrient supply, which suggests an interactive response between these drivers.
76 The molecular catalysts of oxygenic photosynthesis, photosystem II (PSII) and
77 ribulose-1,5-biphosphate carboxylase:oxygenase (RuBisCO), are highly conserved in all
78 photosynthetic organisms (Campbell et al. 2003, Macey et al. 2014) and play a key role in
79 their metabolism and ecophysiology (Li and Campbell 2017). RuBisCO catalyses CO_2
80 fixation (the dark reactions of photosynthesis) and may be the most abundant protein on
81 Earth (Ellis 1979, Bar-On and Milo 2019). Under saturating light, the catalytic rate of
82 RuBisCO often constrains the rate of photosynthesis because it is inefficient (Erb and
83 Zarzycki 2018) and temperature dependent (Geider 1987). PSII binds chlorophyll (as such
84 contributes to the cellular chlorophyll content) and performs the dual role of absorbing light
85 and catalysing the splitting of water, dictating the rate of the light reactions of
86 photosynthesis, which are considered temperature independent (Geider 1987, Ensminger et
87 al. 2006).
88 Toseland et al. (2013) showed that the rate of protein synthesis in eukaryotic
89 phytoplankton increases with temperature. Under nutrient-replete conditions,
90 *Synechococcus* sp. is able to regulate photochemistry over a range of increasing
91 temperatures by increasing the abundance of photosynthetic proteins, including PsbA from
92 PSII, which reflects the need to increase photosynthesis as growth rate increases (Mackey

et al. 2013). Young et al. (2015) found that psychrophilic phytoplankton species, to cope with ambient temperatures that are well below the thermal optimum for most enzymes, increase the abundance of RuBisCO but not of PSII. Under nutrient limitation, resource allocation into photosynthetic proteins can become restricted, resulting in lower growth rates (Falkowski et al. 1989, Halsey and Jones 2015). Given that most studies have investigated the effect of temperature or nutrient supply in isolation, their combined effect upon the photosynthetic machinery remains largely unknown.

The elemental composition and stoichiometry of phytoplankton reflects the changing resource allocation into different macromolecular pools (Moore et al. 2013) and is therefore sensitive to variability in temperature and nutrient supply. The ratio between organic carbon and chlorophyll *a* content (C:Chl*a*) is a central variable in phytoplankton ecophysiology (Geider 1987) that shows consistent patterns in response to abiotic factors, such as an increase with irradiance and a decrease with temperature (Maxwell et al. 1995, Geider 1987, Geider et al. 1997, Halsey and Jones 2015). The ratio between carbon and nitrogen (C:N ratio) can also change in response to environmental variability. However, it has been found to remain relatively constant with temperature under nutrient replete conditions in cultures (Spilling et al. 2015, Yvon-Durocher et al. 2015, Skau et al. 2017) and over a range of different nutrient conditions in the field (Yvon-Durocher et al. 2015, Young et al. 2015), where it was not correlated with temperature. While the variability in C:Chl*a* (Maxwell et al. 1995) and C:N (Moreno and Martiny 2018) ratios as a function of temperature or nutrient supply has been well investigated, changes in stoichiometry due to concurrent variability in both these drivers remain unclear.

Cyanobacteria contribute substantially to both phytoplankton biomass and primary production in the marine environment, particularly when nutrients are limiting (Partensky et

al. 1999). *Synecchococcus* spp. are a significant component of this group (Waterbury et al. 1979), being widely distributed throughout coastal and oceanic environments from the Equator to the high latitudes (Huang et al. 2012, Flombaum et al. 2013), which makes it an appropriate microorganism for studying a wide range of contrasting environmental conditions. To elucidate the interactive effects of temperature and nutrient supply upon the photosynthetic machinery and metabolism of *Synechococcus* sp. we make use of the experiments described by Marañón et al. (2018), in which nitrogen-limited continuous cultures (at dilution rates 0.1 and 0.3 d^{-1}) were maintained at 4 temperatures over the range 18-30 ºC. In addition, we present the results of a new experiment carried out under nutrient-replete conditions over the same temperature range. For all combinations of temperature and nutrient supply, we assessed the resource allocation to photosynthesis and the photosynthetic strategy of the cells by measuring the abundance of the photosynthetic proteins PsbA (PSII protein D1 precursor) and RbcL (RuBisCO large subunit), together with C:N and C:Chl*a* ratios and the rates of photosynthesis, respiration and growth. To link the patterns observed in laboratory with natural variability in the ocean, we also determined variability in RbcL abundance in phytoplankton assemblages across a wide biogeographic gradient covering tropical, temperate and polar regions. Our main goal is to determine the combined role of nutrient availability and temperature in regulating resource allocation, photosynthetic metabolism and growth of *Synechococcus* sp. In particular, we assess the hypothesis that the effect of temperature on photosynthetic protein abundance and metabolic rates (photosynthesis and respiration) is dependent on nutrient availability.

Materials and Methods

We maintained cultures of the marine cyanobacterium *Synechococcus* PCC 7002 (henceforth referred as *Synechococcus*) growing over a range of temperatures from 18 to 30

ºC under contrasting nutrient supply regimes, from strongly nitrogen-limited (N-limited) continuous growth in chemostats to nutrient-replete (N-replete) exponential growth in semicontinuous batch cultures. Steady-state, N-limited chemostats allow the monitoring of populations that are fully acclimated to chronic nutrient limitation and represent the laboratory homologue of the oligotrophic central gyres. N-replete, semicontinuous batch cultures, in contrast, represent near-optimal conditions that simulate transient situations at sea when populations sustain fast growth rates (e.g. blooms). The combination of these constrasting experimental settings thus allowed us to characterize photoautotroph metabolism and growth over a wide ecophysiological gradient.

N-limited chemostat cultures

We maintained *Synechococcus* under N-limited, continuous growth in a Sartorius Biostat Bplus bioreactor, as described by Marañón et al. (2018). To ensure nitrogen limitation of growth, we used a modified f/4 medium with a N:P ratio of 10. The nutrient concentration in the incoming medium was 181.18 µmol nitrate · L^{-1} and 18.12 µmol phosphate · L^{-1}. The dilution rates used, which at steady state equal the population growth rate, were 0.1 d^{-1} and 0.3 d^{-1} and the cultures were maintained at four temperatures for each dilution rate, 18, 22, 26 and 30 ºC ± 0.5 ºC, avoiding supraoptimal temperatures (Mackey et al. 2013). The bioreactor was equipped with two vessels of 2 L and the cultures were aerated with natural air pumped through a 0.45 µm nylon filter. Growth-saturating irradiance (200 µmol photons · m^{-2} · s^{-1}, Six et al. 2004) was provided by LED tubes with a 12:12 (light:dark) photoperiod. After an acclimation period of at least 10 days and when the populations had reached steady-state growth, samples were taken for each combination of temperature and dilution rate. We took samples for the determination of elemental composition, metabolic rates (photosynthesis and respiration) and the abundance of

RuBisCO and D1 protein from photosystem II (proteins encoded by *RbcL* and *PsbA* genes, respectively).

N-replete semicontinuous batch cultures

We grew *Synechococcus* in f/4 medium with a nitrate and phosphate concentration of 441 μmol · L^{-1} and 18 μmol · L^{-1}, respectively. Daily transfer to fresh medium was used to maintain the population under N-replete, exponential growth. Growth temperatures were the same as for the N-limited treatments. We calculated the growth rate (μ) from daily measurements of in vivo fluorescence, as the maximum slope of the linear regression between time and the natural logarithm of fluorescence. The cultures were maintained in 2-L borosilicate round flasks with bubbling air pumped through a 0.45 μm nylon filter. The irradiance conditions were the same as described above for the N-limited cultures. After an acclimation period of at least 10 days, we obtained samples for elemental composition, metabolic rates, and RbcL and PsbA abundance.

Chlorophyll a (Chla) and particulate organic matter

In vivo fluorescence was measured daily with a TD-700 Turner fluorometer (Turner Designs, San Jose, CA, USA). We also determined Chl*a* concentration fluorometrically on 5-mL samples filtered through 25-mm diameter GF/F Whatmann filters, stored at -20 ºC and extracted with 90% acetone overnight. Particulate organic carbon (POC) and nitrogen (PON) were determined on duplicate 10-mL samples filtered through pre-combusted 25-mm of diameter GF/F filters and stored at -20 ºC. Filters were dried at room temperature for 48 hours and then analysed with a Carlo Erba Instruments EA 1108 elemental analyser.

Photosynthetic protein analyses

Culture samples (20-300 mL in volume) were filtered onto 0.2-μm polycarbonate filters, which were transferred to cryovials, flash-frozen with liquid nitrogen and stored at -

80 ºC. For protein extraction, 500 µL of denaturation protein extraction buffer was added to each filter (140 mM Tris base, 105 mM Tris-HCl 0.5 mM EDTA, 2% lithium dodecyl sulphate, 10% glycerol, and 0.1 mg · mL^{-1} PefaBloc SC protease inhibitor (Merck, Darmstadt, Germany)). The filters were then flash-frozen in liquid nitrogen and total protein was extracted using 4 rounds of sonication with a Vibra-Cell Ultrasonic Processor with a micro-tip attachment (Sonics and Materials, Newton, CT, USA), as described by Brown et al. (2008). To avoid over-heating, between each round of sonication, samples were refrozen immediately in liquid nitrogen. The total protein concentration of the extracts was determined using the BCA protein assay (Pierce, Thermo Fisher Scientific, Waltham, MA, USA). The abundance of RuBisCO, here represented as the large subunit encoded by the *RbcL* gene, and the D1 protein, core reaction centre of photosystem II encoded by the *PsbA* gene, was determined by Western Blotting. Total protein extracts (1-2 µg total protein) were separated by SDS-PAGE alongside a series of 3-4 RbcL or PsbA protein standards (Agrisera, Vännäs, Sweden) of known concentration on 1.5-mm NuPAGE Bis-Tris 4-12% acrylamide gradient mini-gels with 1X MES running buffer (Invitrogen, Thermo Fisher Scientific, Waltham, MA, USA). Gels were run in an XCell Sure-Lock Tank (Invitrogen) at 200 V for 35 minutes. The separated proteins were transferred to a polyvinyl difluoride (PVDF) membrane pre-wetted with methanol and equilibrated in 1X NuPAGE Transfer Buffer (Invitrogen) containing 10% methanol. Transfers were run in an XCell blot module (Invitrogen) at 30V for 55 minutes (PsbA) or 70 minutes (RbcL). Blots were probed with polyclonal, global anti-PsbA or anti-RbcL primary antibodies (1:40000 *PsbA*; 1:30000 *RbcL*) (Abcam, Cambrigge, UK) as described by Brown et al. (2008). Blots were developed with Amersham ECL Select Western Blotting Detection Reagent (GE Healthcare Life Sciences, Buckinghamshire, UK) and imaged with a LI-COR C-DiGit blot

scanner (LI-COR Biosciences, Cambridge, UK). Band intensities for protein standards and samples were quantified using Image J (Schneider et al. 2012).

Protein standard band intensities were plotted as standard curves and used to estimate PsbA and RbcL quantities in the loaded samples. Results were only used when samples fell within the linear range of the loaded standards.

The abundance of both RbcL and PsbA were expressed in pmol · (µg total protein)$^{-1}$ and as a weight percentage relative to total protein. For the latter, we took into account that *Synechococcus* contains Form 1 RuBisCO with eight equimolar subunits per molecule (RbcL and RbcS). Picomoles of RbcL were converted to µg of RbcL using the molecular weight of 52.159 kDa (UniProt ID Q44176) and µg of RbcS were calculated using equimolar pmol and a molecular weight of 13.212 kDa (UniProt ID Q44178). The D1 core reaction centre of PSII, PsbA, has a molecular weight of 39.711 kDa (UniProt ID B1XM24) and µg of the samples were calculated directly from the pmol quantities measured on the Western Blots. Finally, concentration of both proteins, RuBisCO and PsbA, were expressed as a percentage of the total protein (µg) loaded onto the gel.

In situ RuBisCO abundance

To complement the laboratory experiments we included 65 samples that had been collected from surface waters during three different cruises spanning polar, temperate and tropical latitudes (64˚N to 78˚S), thus covering a wide range of environmental conditions including temperature and nutrient availability: (1) 26 samples from the *RVIB Nathaniel B. Palmer* cruise to the Ross Sea (cruise NBP12-01, 72-78°S, 160°W-160°E; see Ryan-Keogh et al. 2017) from 24th December 2011 to 10th February 2012; (2) 16 samples for the *RRS Discovery* cruises to the subpolar North Atlantic, a spring cruise (cruise D350, 58-63°N, 16-36°W; see Ryan-Keogh et al. 2013) from 28th April to 10th May 2010 and a summer

cruise (cruise D354, 56-64°N, 8-42°W; see Ryan-Keogh et al. 2013) from 4th July to 10th August 2010; and (3) 23 samples for the *RRS James Cook* AMT19 cruise (Atlantic Meridional Transect, 50°N to 47°S) from 13th October to 1st December 2009. In all cases, whole seawater was collected from Niskin bottles on a CTD rosette system from 5 metres depth. Samples for protein extraction were collected by filtering 1.0-3.0 L of seawater onto GF/F Whatman filters under low light for ~45 minutes to minimize changes in protein abundance following sampling. Filters were flash-frozen and stored at -80 °C until analysis. RbcL protein abundance, used as a proxy of RuBisCO abundance, was quantified using the techniques described above (Brown et al., 2008). The abundance of RbcL was expressed in pmol (μg total protein)$^{-1}$ using the molecular weight of RbcL as described above.

Metabolic rates

Rates of photosynthesis and respiration were determined with the O_2-evolution technique. Eight gravimetrically-calibrated and acid-washed, borosilicate glass bottles of 30 mL in volume were filled with culture. Two replicate bottles were fixed immediately for initial oxygen concentration and the other six bottles were incubated for 2.5 h in a temperature-controlled chamber. Three bottles were incubated in darkness and the other three were incubated under the same irradiance conditions experienced by the cultures. Dissolved oxygen concentration was measured with the Winkler technique using a potentiometric endpoint. To obtain the metabolic rates in units of carbon, we applied a molar O_2 to CO_2 ratio of 1.4 (Laws 1991).

Carbon-specific photosynthesis (P^C) and respiration (R^C) were calculated by dividing hourly metabolic rates by POC concentration, while chlorophyll *a*-specific photosynthesis (P^{Chla}) was calculated by dividing the photosynthesis rate by Chl*a* concentration.

Data treatment and statistical analyses

We used linear regression analyses to assess the effect of temperature and nutrient supply upon photosynthetic protein abundance, elemental stoichiometry, and metabolic rates. Normalisation was required to remove the effect of either temperature or nutrient supply and analyse the effect of the other driver in isolation. Normalisation of a given variable was conducted by dividing each value by the mean value for the corresponding nutrient or temperature treatment. Growth rate was used as a common metric for nutrient supply in both N-limited and N-replete cultures. The non-parametric Kruskal-Wallis *H* test was used to assess differences among temperatures within a given nutrient treatment, followed by a Dunn-Bonferroni's post-hoc comparison test to ascertain which temperature treatments differed.

We quantified the effect of temperature on metabolic rates and, for the N-replete treatment, on growth rate by calculating the activation energy (E_a). Ordinary least-squares regression was used to determine the slope ($-E_a$) of the linear relationship between $1/KT$ (where K is Boltzmann's constant and T is temperature in °K) and the natural logarithm of carbon-specific metabolic rate or growth rate. Since there was no differential effect of temperature upon photosynthesis and respiration rates in the 0.1 and 0.3 d^{-1} treatments, in these analyses we pooled together the data from both of the nutrient-limited treatments. Thus, we considered only two nutrient conditions, N-replete and N-limited, obtaining a single value of E_a for each one. All statistical analyses were carried out with SPSS v. 22 and R Studio v. 3.5.1.

Results

Abundance of photosynthetic proteins

The abundance of RuBisCO and PsbA in our experiments, expressed as a percentage of total protein, ranged between 0.3-1.7 and 0.01-0.23%, respectively (Fig. 1), which corresponds to an abundance of 0.05-0.25 pmol · (μg total protein)$^{-1}$ for RbcL and 0.003-0.058 pmol · (μg total protein)$^{-1}$ for PsbA (see Table S1 in Supporting Information). Both proteins increased their abundance from the N-limited treatments to the N-replete one by at least a factor of two. In the N-replete treatment, RuBisCO abundance (Fig. 1a) reached 1.7% at the coldest temperature and values around 1.0% for the other 3 temperatures. In contrast, RuBisCO abundance was lower in the N-limited treatments, with a mean value of 0.45% at 0.1 d^{-1} and 0.36% at 0.3 d^{-1}. PsbA abundance was lower than that of RuBisCO (Fig. 1b) but increased more markedly with increasing nutrient supply, from a mean value of 0.02% at 0.1 d^{-1} N-limited treatment to 0.08 at 0.3 d^{-1} and 0.19 in the N-replete treatment. Irrespective of temperature, PsbA and RuBisCO abundance increased with nutrient-dependent growth rate ($R^2 = 0.85$, n = 12, $p < 0.01$ and $R^2 = 0.58$, n = 12, $p < 0.01$, respectively, Table S2).

There was a significant effect of temperature on the abundance of PsbA in the N-replete and 0.3 d^{-1} N-limited treatments (Fig. 1b), as shown by the regression between temperature and normalised PsbA content ($R^2 = 0.84$, n = 8, $p < 0.01$, Fig. S1). In contrast, temperature did not affect PsbA abundance in the 0.1 d^{-1} N-limited treatment nor did it consistently affect RuBisCO abundance in any of the nutrient treatments. The only exception to this pattern was the N-replete treatment, in which RuBisCO abundance was significantly different among temperatures ($\chi^2 = 8.82$, n = 16, df = 3, $p = 0.03$), showing significantly higher values at 18 °C (*ca*. 50%) than those of all other temperatures (post-hoc Dunn-Bonferroni's test). Due to the strong effect of nutrient supply on total protein abundance, there was a significant, positive correlation between the abundance of each

protein (Spearman's r = 0.6, $p < 0.05$, n = 12, Fig. 2).

PsbA abundance was particularly sensitive to nutrient limitation and as a consequence the PsbA:RbcL ratio in the 0.1 d^{-1} treatment (<0.15) was lower than in the 0.3 d^{-1} and N-replete treatments (0.15-0.45, Fig. S2). The PsbA:RbcL ratio increased with temperature in the N-replete treatment, but did not show any consistent pattern with temperature under nutrient limitation.

The RbcL to chlorophyll *a* ratio tended to increase with decreasing temperature both in the N-replete treatment and the 0.1 d^{-1} N-limited treatment, while showing no consistent relationship with increasing nutrient supply (Table S1, Fig. S3). The PsbA:Chl*a* ratio showed a comparatively smaller degree of variability, and did not show any clear pattern of response to either temperature or nutrient supply (Fig. S3).

In situ data showed that the abundance of RbcL, relative to both total protein and total chlorophyll *a* content, increased markedly with decreasing seawater temperature, an effect that was particularly evident for temperatures below 10 ˚C (Fig. 3). For the ensemble of the 65 samples analysed, RbcL abundances ranged between 0.01-0.12 pmol · (µg total protein)$^{-1}$ and 1.5-111 mmol · (mol Chl*a*)$^{-1}$.

Cellular composition

The molar carbon to nitrogen ratio of particulate organic matter (C:N) ranged between 5 and 13, with the lowest values being measured in the N-replete treatments (Fig. 4a). There was a significant effect of nutrient supply on the normalised C:N ratio (R^2 = 0.57, n = 12, $p < 0.01$, Table S2), whereas temperature explained a smaller amount of variability (R^2 = 0.42, n = 12, $p < 0.05$, Table S2). C:Chl*a,* which ranged between 39 and 215 µg C:µg Chl*a,* tended to decrease with increasing nutrient supply and temperature (Fig. 4b). Regardless of the temperature considered, C:Chl*a* was 50-100% higher in the 0.1 d^{-1}

332 treatment than in the N-replete one. There was also a strong effect of temperature on
333 C:Chl*a*, which, over the 18 to 30 °C range, decreased from 215 to 137 at 0.1 d^{-1}, from 134
334 to 51 at 0.3 d^{-1} and from 165 to 39 in the N-replete treatment, resulting in a significant
335 linear relationship between temperature and normalised C:Chl*a* ($R^2 = 0.68$, n = 12, $p <$
336 0.01).
337 *Metabolic rates and growth*
338 P^C increased markedly with increasing nutrient supply (Fig. 5a), taking mean values
339 from 0.02 h^{-1} at 0.1 d^{-1} to 0.03 at 0.3 d^{-1} and 0.09 h^{-1} in the N-replete treatment.
340 Temperature had a strong effect in the N-replete treatment, where P^C increased 2-fold with
341 increasing temperature, from 0.06 h^{-1} at 18 ºC to 0.12 h^{-1} at 30 ºC, but not in the N-limited
342 treatments, where P^C remained largely constant over the assayed temperature range. E_a for
343 photosynthesis was 0.32 eV in the N-replete treatment and 0.02 under N-limited growth,
344 whereas E_a for growth rate under N-replete conditions was 0.49 eV (Table 1, Fig. 6).
345 $P^{Chl\,a}$ had values in the range 1.5-10 µgC · µgChla^{-1} · h^{-1} for the ensemble of all temperature
346 and nutrient supply treatments (Fig. 5b). $P^{Chl\,a}$ took much higher values under N-replete
347 conditions than in the N-limited treatment. After normalising to remove the effect of
348 temperature, nutrient supply explained almost half of the variability in $P^{Chl\,a}$ ($R^2 = 0.45$, n =
349 12, $p < 0.05$). $P^{Chl\,a}$ responded stronger to changes in temperature, decreasing by
350 approximately 50% with increasing temperature over the 18 to 30 °C range ($R^2 = 0.84$, n =
351 12, $p < 0.01$, Table S2). R^C took values between 0.001 and 0.008 h^{-1} (Fig. 5c) and did not
352 show a clear response to nutrient supply. R^C increased markedly with temperature only in
353 the N-replete treatment ($E_a = 1.6$), whereas it was relatively constant in both of the N-
354 limited treatments.
355

Discussion

Variability in photosynthetic protein abundance

Our experimental design serves to quantify the range of variability in key photosynthetic proteins across a relatively wide range of environmental conditions. The abundance of RbcL and PsbA ranged between 0.05-0.25 and 0.003-0.06 pmol · (µg total protein)$^{-1}$, respectively, which corresponds to a relative protein content of 0.3-1.7% for RuBisCO and 0.01-0.2% for PsbA. These ranges coincide with previous reports of protein abundance in both natural communities and cultures. For instance, Losh et al. (2012) investigated the effect of CO_2 and nutrient limitation upon phytoplankton stoichiometry and photophysiology in the California Current and found that the abundance of RbcL ranged between 0.03 and 0.20 pmol · (µg total protein)$^{-1}$, while that of PsbA fell within the range 0.01-0.04 pmol · (µg total protein)$^{-1}$. The abundance of RuBisCO in batch cultures of eight microalgae growing under various conditions of nutrient and CO_2 availability ranged between 0.5-6% (Losh et al. 2013). Higher protein contents were found by Li and Campbell (2017), who assessed the effect of different nutrient regimes and growth irradiances in two diatom species and reported abundances in the range 0.7-3 pmol · (µg total protein)$^{-1}$ for RbcL and 0.04-0.1 pmol · (µg total protein)$^{-1}$ for PsbA.

Effect of temperature and nutrients on RuBisCO and PsbA

Losh et al. (2012, 2013) found that RbcL and PsbA content increased with increasing nutrient supply, whereas Li and Campbell (2017) reported that cells growing under N limitation increased their cellular allocation to RuBisCO and PsbA. Our results agree with those of Losh et al. (2012, 2013), as we measured the highest protein contents in the N-replete treatment, irrespective of temperature. Our results also show a positive relationship, already seen in previous studies, between growth rate and RuBisCO

abundance (Falkowski et al. 1989, Raven 1991, Losh et al. 2012, 2013, Young et al. 2015) and between growth rate and PsbA abundance (Macey et al. 2014, Ryan-Keogh et al. 2017).

In our experiments, temperature had a more modest effect on protein abundance than nutrient supply. Furthermore, the effect of temperature was more noticeable under high nutrient supply. Increasing temperature enhanced the abundance of PsbA under N-replete conditions, but not under N-limitation. These results support our initial hypothesis that the effect of temperature on photosynthetic metabolism is, in turn, dependent on nutritional status. In contrast, increased temperature did not result in enhanced RuBisCO abundance. This pattern may arise because the light reactions catalysed by PSII are temperature independent, whereas dark reactions, such as CO_2-fixation by RuBisCO, are temperature-dependent (Geider 1987). Under high resource supply (N-replete, light-saturated growth), increasing temperature leads to faster RuBisCO turnover and higher CO_2 fixation rates, so additional capacity of the PSII light reactions is required to provide the reductants and energy needed for carbon-fixation (Ensminger et al. 2006). Conversely, under strong nutrient limitation cells can no longer invest in protein catalysts, such that protein abundance and biosynthetic rates become temperature-insensitive (O'Connor et al. 2009, Marañón et al. 2018) and, in the case of our N-limited *Synechococcus* population, photosynthetic rates remain constant with temperature. This, then, would explain the lack of change in PsbA abundance with temperature when nutrients are limiting.

Psychrophilic diatoms invest more resources in RuBisCO when temperatures are suboptimal (Young et al. 2015). These authors found that elevated carbon fixation rates during blooms in polar regions are associated with RuBisCO protein content as high as 17%. In our experiments, we observed a significant increase in RuBisCO abundance at 18

ºC (the lowest tested temperature) only in the N-replete treatment. Given that 18 ºC is well below the thermal optimum for both the RuBisCO carboxylase activity (Galmés et al. 2013) and for the growth rate of this tropical isolate specie (Mackey et al. 2013), the increased RuBisCO abundance at this temperature might represent an acclimation response to compensate for its decreased catalytic rate.

Although RuBisCO only constitutes a small percentage of total protein N (Macey et al. 2014, Young et al. 2015), similar temperature sensitivities for other photosynthetic and non-photosynthetic enzymes may combine to explain why the increase in RuBisCO abundance was found only under N-replete conditions. Overall, these results suggest a preferential resource allocation into PSII instead of RuBisCO as temperature rises, mostly under N-replete conditions, which also supports the existence of an interactive effect between temperature and nutrients that controls the abundance of these photosynthetic proteins.

In situ RuBisCO variability and phytoplankton photosynthetic strategies

Our measurements of in situ RuBisCO abundance allow us to examine if the responses observed in laboratory monocultures can be extrapolated to multispecific phytoplankton assemblages in the field. Conversely, the patterns identified in the laboratory experiments can illuminate the mechanisms underlying the variability in RuBisCO abundance along a wide biogeographic gradient. The temperature range spanned by the in situ samples (0-27 °C) is much wider than that of the laboratory experiments and, as it covers tropical, temperate and polar regions, is associated with large changes in species composition and functional traits (Barton et al. 2013). Yet, it is remarkable that the pattern of increased RbcL abundance (relative to both total protein and Chl*a*) associated with cold temperatures was consistent between laboratory and in situ observations. These results

suggest a phytoplankton photosynthetic strategy that is similar across single-taxon acclimation and community acclimation and adaptation, whereby the relative abundance of RuBisCO increases at low temperature to overcome the lower catalytic rates of this temperature-dependent enzyme (Young et al. 2015). This low-temperature strategy, however, implies an increased requirement for nitrogen, which explains that the enhanced RuBisCO abundance was found only in polar regions (<10 ºC), which are nitrogen-rich environments (Moore et al. 2013). As temperature increases, phytoplankton invest relatively more resources in the light reactions of photosynthesis (i.e. chlorophyll *a*, PSII) to provide the required energy and reductant for the cell. If nutrients are not limiting, at high temperature the increase in Chl*a* to RuBisCO and PsbA to RuBisCO ratios could reflect the increased need to provide the now more efficient RuBisCO with the required reductant and energy needed for carbon fixation. Where nutrients are limiting at higher temperatures there may also be an increased uncoupling between the light and dark reactions of photosynthesis as energy and reductant is used in nutrient uptake and cellular maintenance rather than carbon fixation (Hughes et al. 2018).

Variability in C:N and C:Chla ratios

The elemental composition of phytoplankton reflects the patterns of resource allocation into subcellular components and constitutes a critical factor that regulates nutrient cycling, primary production and energy transfer through marine food webs (Raven and Geider 1988, Arrigo 2005, Moreno and Martiny 2018). Our results demonstrate that C:N ratio in *Synechococcus* is strongly dependent on nutrient supply, showing lower values associated with increasing growth rates and protein content. In contrast, C:N showed only a slight increase with temperature under N-limited conditions while showing no response to temperature under N-replete growth, as has been shown before for multiple phytoplankton

452 species (Yvon-Durocher et al. 2015).

453 The C:Chl*a* ratio was strongly regulated by both nutrient supply and temperature.
454 Phytoplankton adjust their chlorophyll *a* content in response to nutrient availability because
455 the photosynthetic machinery accounts for a high fraction of cellular nitrogen (Eppley
456 1972, Halsey et al. 2010, Halsey and Jones 2015). Strong nutrient limitation (represented in
457 our experiments by the 0.1 d^{-1} dilution rate) causes a reduction in the synthesis of pigment-
458 protein complexes (including PSII), which ultimately leads to high C:Chl*a* ratios associated
459 with slow growth. The C:Chl*a* ratio also increases with decreasing temperature, irrespective
460 of the nutrient treatment. The inverse relationship between temperature and pigment
461 content is a well-established pattern in phytoplankton and higher plants, which may result
462 from an adaptive strategy to attain a balance between the temperature-dependent dark
463 reactions involved in carbon fixation and the temperature-independent light reactions
464 (Geider 1987). At the molecular level, acclimation to high temperature mimics acclimation
465 to low irradiance, as in both cases light-harvesting capacity and the catalysts of the light
466 reactions of photosynthesis (i.e. PSII) are increased to maintain the supply of energy and
467 reductant to the dark reactions for carbon fixation (Maxwell et al. 1995).

468 *Effect of temperature and nutrients on metabolic rates and growth*

469 As in the case of protein abundance, the interactive effect between temperature and
470 nutrient supply also applied to metabolic rates. Both photosynthesis and respiration
471 increased with temperature only under nutrient-replete conditions, while being largely
472 temperature-independent in the nutrient-limited treatments. The E_a values measured in our
473 N-replete cultures for photosynthesis, respiration and growth rates were within the range of
474 E_a values previously reported for picoplankton (Chen et al. 2014). The estimate of E_a for
475 growth rate (0.49 eV) is higher than the value predicted by the metabolic theory of ecology

for photosynthetic organisms (0.32 eV; Allen et al. 2005), which supports the emerging view that the difference in temperature dependence of growth under nutrient-sufficient conditions between autotrophic and heterotrophic planktonic unicells may be smaller than previously assumed (Chen and Laws 2016, Wang et al. 2018).

Chlorophyll *a*-specific photosynthesis is commonly used to assess the metabolic responses of phytoplankton to environmental drivers, and is a key component in bio-optical models of marine productivity, but the interpretation of its variability is complicated by the fact that CO_2 fixation and Chl*a* content (both expressed per unit of carbon biomass) can change markedly as growth conditions vary. Previous studies have shown that $P^{Chl\,a}$ increases with temperature in several species of unicellular photoautotrophs, including cyanobacteria (Fu et al. 2007, Spilling et al. 2015), although there are also reports showing that it can remain stable or even decrease with increasing temperature (Tang and Vincent 2000). In our experiments, $P^{Chl\,a}$ consistently decreased with temperature in all nutrient supply treatments. One possible explanation is that, as a result of increased intracellular Chl*a* content, cells growing under warmer temperatures experienced a decrease in Chl*a*-specific light absorption (*a**), i.e. an enhanced package effect, as observed before in cultures of cyanobacteria and chlorophytes (Sosik and Mitchell 1994, Yin et al. 2016).

Conclusions

Changes in nutrient supply have a larger effect than temperature on photosynthetic protein abundance and metabolism of *Synechococcus*. The effects of temperature upon the photosynthetic machinery, metabolic rates and biochemical composition are dependent on nutrient availability. Our results suggest that resource allocation into PSII and chlorophyll *a* (representing the light reactions of photosynthesis) increases with temperature, mainly under nutrient-replete conditions, to balance the presumably enhanced specific catalytic

activity of RuBisCO. Low temperatures together with high nutrient availability cause an increased investment in RuBisCO, a pattern that is observed also in natural phytoplankton assemblages across a wide latitudinal range. The response of photosynthesis and respiration rates of *Synechococcus* to increasing temperature is strong (E_a between 0.3-1.6 eV) only under nutrient-sufficient conditions, not under nutrient limitation. These findings contribute to improve our mechanistic understanding of how the biochemical composition, photophysiology and metabolism of this ubiquitous and biogeochemically relevant marine cyanobacterium responds to environmental variability.

Acknowledgments

This research was supported by the Spanish Ministry of Science and Innovation through research grant PGC2018-094553-B-I00 to E. M. We thank the scientific complement and crew of the RRS James Cook, RVIB Nathaniel B. Palmer and RRS Discovery during AMT-19, NBP12-01, D350 and D354 respectively, for all of their assistance. These cruises were supported by grants from the National Science Foundation, USA (ANT-0944254) and National Environmental Research Council, UK (NE/F019254/1 and NE/G009155/1). C. F.-G. acknowledges the receipt of a predoctoral research fellowship from Xunta de Galicia. We thank Ángeles Saavedra for advice with statistical analyses and M. J. Cabrerizo for comments on an earlier version of the manuscript

Author contribution

Author contributions were as follows: C. F.-G, T. S. B., C. M. M. and E. M. designed the study, analysed the data, and wrote the manuscript; C. F.-G., M. P.-L. and N. P. obtained samples and data; all authors commented on the manuscript.

References

Allen, A. P., Gillooly, J. F., Brown, J. H. 2005. Linking the global carbon cycle to individual metabolism. Funct. Ecol. 19:202–213

Arrigo, K. R. 2005. Marine microorganisms and global nutrient cycles. *Nature* 437:349–355

Bar-On, Y. M., Milo, R. 2019. The global mass and average rate of rubisco. *PNAS U.S.A*. doi: i/10.1073/pnas.1816654116

Barton, A. D., Pershing, A. J., Litchman, E., Record, N. R., Edwards, K. F., Finkel, Z. V., Kiørboe, T., Ward, B. A. 2013. The biogeography of marine plankton traits. Ecol. Lett. 16:522-534

Brown, C. M., MacKinnon, J. D., Cockshutt, A. M., Villareal, T. A., Campbell, D. A. 2008. Flux capacities and acclimation costs in *Trichodesmium* from the Gulf of Mexico. Mar. Biol. 154:413–422

Campbell, D. A., Cockshutt, A. M., Porankiewicz-Asplund, J. 2003. Analysing photosynthetic complexes in uncharacterized species or mixed microalgal communities using global antibodies. Physiol. Plant. 119:322–327

Chen, B., Laws, E. A. 2016. Is there a difference of temperature sensitivity between marine phytoplankton and heterotrophs? Limnol. Oceanogr. 62:806–817

Chen, B., Liu, H., Huang, B., Wang, J. 2014. Temperature effects on the growth rate of marine picoplankton. Mar. Ecol. Prog. Ser. 505:37–47

Cross, W. F., Hood, J. M., Benstead, J. P. 2015. Interactions between temperature and nutrients across levels of ecological organization. Glob. Chang. Biol. 21:1025–1040

Doney, S. C., Ruckelhaus, M., Duffy, J. E., Barry, J. P., Chan, F., English, C. A., Galindo, H. M., Grebmeier, and others. 2014. Climate Change Impacts on Marine Ecosystems. Annu. Rev. Mar. Sci. 4:11-37

Erb, T. J., Zarzycki, J. 2018. A short history of RubisCO: the rise and fall (?) of Nature's predominant CO_2 fixing enzyme. Curr. Opin. Biotechnol. doi: 10.1016/j.copbio.2017.07.017

Ellis, R. J. 1979. The most abundant protein in the world. Trends Biochem. Sci. 4:241–244

Ensminger, I., Busch, F., Huner, N. P. A. 2006. Photostasis and cold acclimation: sensing low temperature through photosynthesis. Physiol. Plant. 126:28–44

Eppley, R. W. 1972. Temperature and phytoplankton growth in the sea. Fish. Bull. 10:1063–1085

Falkowski, P. G., Sukenik, A., Herzig, R. 1989. Nitrogen limitation in *Isochrysis Galbana* (Haptophyceae) II. Relative abundance of chloroplast proteins. J.Phycol. 25:471–478

Flombaum, P., Gallegos, J. L., Gordillo, R. A., Rincon, J., Zabala, L. L., Jiao, N., Karl, D. M., Li, and others. 2013. Present and future global distributions of the marine Cyanobacteria *Prochlorococcus* and *Synechococcus*. PNAS U.S.A. 110:9824–9829

Fu, F. X., Warner, M. E., Zhang, Y., Feng, Y., Hutchins, D. A. 2007. Effects of increased temperature and CO_2 on photosynthesis, growth, and elemental ratios in marine *Synechococcus* and *Prochlorococcus* (Cyanobacteria). J. Phycol. 43:485–496

Galmés, J., Aranjuelo, I., Medrano, H., Flexas, J. 2013. Variation in Rubisco content and activity under variable climatic factors. Photosynth. Res. 117:73–90

Geider, R. J. 1987. Light and temperature dependence of the carbon to chlorophyl a ratio in microalgae and Cyanobacteria: implications for physiology and growth of phytoplantkon. New Phytol. 106:1–34

Geider, R. J., Macintyre, H. L., Kana, T. M. 1997. Dynamic model of phytoplankton growth and acclimation: Responses of the balanced growth rate and the chlorophyll*a*:carbon ratio to light, nutrient-limitation and temperature. Mar. Ecol. Progr. Ser. 148:187–200

Halsey, K. H., Jones, B. M. 2015. Phytoplankton strategies for photosynthetic energy allocation. Ann. Rev. Mar. Sci. 7:265–297

595 Halsey, K. H., Milligan, A. J., Behrenfeld, M. J. 2010. Physiological optimization underlies
596 growth rate-independent chlorophyll-specific gross and net primary production.
597 Photosynth. Res. 103:125–137
598
599 Huang, S., Wilhelm, S. W., Harvey, H. R., Taylor, K., Jiao, N., Chen, F. 2012. Novel
600 lineages of *Prochlorococcus* and *Synechococcus* in the global oceans. ISME J. 6:285–297
601
602 Hughes, D. J., Varkey, D., Doblin, M. A., Ingleton, T., Mcinnes, A., Ralph, P.J., Dongen-
603 Vogels, V. V., Suggett, D. J. 2018. Impact of nitrogen availability upon the electron
604 requirement for carbon fixation in Australian coastal phytoplankton communities. Limnol.
605 Oceanogr. 63:1891–1910
606
607 Laws, E. A. 1991. Photosynthetic quotiens, new production and net community production
608 in the open ocean. Deep-Sea Res. 38:143-167
609
610 Lewandowska, A. M., Boyce, D. G., Hofmann, M., Matthiessen, B., Sommer, U., Worm,
611 B. 2014. Effects of sea surface warming on marine plankton. Ecol. Lett. 17:614–623
612
613 Li, G., Campbell, D. A. 2017. Interactive effects of nitrogen and light on growth rates and
614 RUBISCO content of small and large centric diatoms. Photosynth. Res. 131:93-103
615
616 Losh, J. L., Morel, F. M. M., Hopkinson, B. M. 2012. Modest increase in the C:N ratio of
617 N-limited phytoplankton in the California Current in response to high CO_2. Mar. Ecol.
618 Progr. Ser. 468:31–42

Losh, J. L., Young, J. N., Morel, F. M. M. 2013. Rubisco is a small fraction of total protein in marine phytoplankton. New Phytol. 198:52–58

Ludwig, M., Bryant, A. D. 2012. Acclimation of the global transcriptome of the cyanobacterium *Synechococcus* sp. strain PCC 7002 to nutrient limitations and different nitrogen sources. Front. Microbiol. 3:145 doi: 10.3389/fmicb.2012.00145

Macey, A. I., Ryan-Keogh, T., Richier, S., Moore, C. M., Bibby, T. S. 2014. Photosynthetic protein stoichiometry and photophysiology in the high latitude North Atlantic. Limnol. Oceanogr. 59:1853–1864

Mackey, K. R. M., Paytan, A., Caldeira, K., Grossman, A. R., Moran, D, McIlvin, M., Saito, M. A. 2013. Effect of temperature on photosynthesis and growth in marine *Synechococcus* spp. Plant Physiol. 163:815–829

Marañón, E., Cermeño, P., Huete-Ortega, M., López-Sandoval, D. C., Mouriño-Carballido, B., Rodríguez-Ramos, T. 2014. Resource supply overrides temperature as a controlling factor of marine phytoplankton growth. PLoS One 9:20–23

Marañón, E., Lorenzo, M. P., Cermeño, P., Mouriño-Carballido, B. 2018. Nutrient limitation suppresses the temperature dependence of phytoplankton metabolic rates. ISME J. 12:1836–1845

643 Maxwell, D. P., Laudenbach, D. E., Huner, N. P. A. 1995. Redox regulation of light-
644 harvesting complex II and cab mRNA abundance in *Dunaliella salina*. Plant Physiol.
645 109:787–795
646
647 Moore, C. M., Mills, M. M., Arrigo, K. R., Berman-Frank, I., Bopp, L., Boyd, P. W.,
648 Galbraith, E. D., Geider, R. J., Guieu, C., Jaccard, S. L. and others. 2013. Processes and
649 patterns of oceanic nutrient limitation. Nat Geosci. 6:701–710
650
651 Morán, X. A. G., Calvo-Díaz, A., Arandia-Gorostidi, N., Huete-Stauffer, T. M. 2018.
652 Temperature sensitivities of microbial plankton net growth rates are seasonally coherent
653 and linked to nutrient availability. Environ. Microbiol. 20:3798–3810
654
655 Moreno, A. R., Martiny, A. C. 2018. Ecological stoichiometry of ocean plankton. Annu.
656 Rev. Mar. Sci. 10:43–69
657
658 O'Connor, M. I., Piehler, M. F., Leech, D. M., Anton, A., Bruno, J. F. 2009. Warming and
659 resource availability shift food web structure and metabolism. PLoS Biology
660 doi:10.1371/journal.pbio.1000178
661
662 Partensky, F., Blanchot, J., Vaulot, D. 1999. Differential distribution and ecology of
663 *Prochlorococcus* and *Synechococcus* in oceanic waters: a review. Bull. Inst. Ocenogr.
664 19:457–475
665
666 Raven, J. A. 1991. Physiology of inorganic C acquisition and implications for resource use

667 efficiency by marine phytoplankton: relation to increased CO_2 and temperature. Plant. Cell.
668 Environ. 14:779–794
669
670 Raven, J. A., Geider, R. J. 1988. Temperature and algal growth. New Phytol. 110:441–461
671
672 Ryan-Keogh, T. J., Macey, A. I., Nielsdóttir, M. C., Lucas, M. I., Steigenberger, S. S.,
673 Stinchcombe, M. C., Achterberg, E. P., Bibby, T. S., and others. 2013. Spatial and temporal
674 development of phytoplankton iron stress in relation to bloom dynamics in the high-latitude
675 North Atlantic Ocean. Limnol. Oceanogr. 58(2):533-545
676
677 Ryan-Keogh, T. J., DeLizo, L. M., Smith, W. O., Sedwick, P. N., McGillicuddy, D. J.,
678 Moore, C. M., Bibby, T. S. 2017. Temporal progression of photosynthetic-strategy in
679 phytoplankton in the Ross Sea, Antarctica. J. Mar.Syst. 166:87–96
680
681 Schneider, C. A., Eliceiri, K., Rasband, W. S., Eliceiri, K.W. 2012. NIH Image to ImageJ:
682 25 years of image analysis. Nat. Methods. 9:671–675
683
684 Six, C., Thomas, J., Brahamsha, B., Lemoine, Y., Partensky, F. 2004. Photophysiology of
685 the marine cyanobacterium *Synechococcus* sp. WH8102, a new model organism. Aquat.
686 Microb. Ecol. 35:17–29
687
688 Skau, L. F., Andersen, T., Thrane, J-E., Hessen, D. O. 2017. Growth, stoichiometry and cell
689 size; temperature and nutrient responses in haptophytes. Peer J. doi:10.7717/peerj.3743

690

691 Sosik, H. M., Mitchell, G. B. 1994. Effects of temperature on growth, light absorption, and
692 quantum yield in *Dunaliella tertiolecta* (Chlorophyceae). J. Phycol. *30:8*33-840

693

694 Spilling, K., Ylöstalo, P., Simis, S., Seppälä, J. 2015. Interaction effects of light,
695 temperature and nutrient limitations (N, P and Si) on growth, stoichiometry and
696 photosynthetic parameters of the cold-water diatom *Chaetoceros wigham*ii. PLoS One
697 10:1–18

698

699 Tang, E., Vincent, W. 2000. Effects of daylength and temperature on the growth and
700 photosynthesis of an arctic cyanobacterium, Schizothrix calcicola (Oscillatoriaceae). Eur. J.
701 Phycol. 35:263–272

702

703 Toseland, A., Daines, S. J., Clark, J. R., Kirkham, A., Strauss, J., Uhlig, C., Lenton, T. M.,
704 Valentin, K., and others. 2013. The impact of temperature on marine phytoplankton
705 resource allocation and metabolism. Nat. Clim. Change 3:979–984

706

707 Wang, Q., Lyu, Z., Omar, S., Cornell, S., Yang, Z., Montagnes, D. J. S. 2018. Predicting
708 temperature impacts on aquatic productivity: Questioning the metabolic theory of ecology's
709 "canonical" activation energies. Limnol. Oceanogr. 9999:1–14

710

711 Waterbury, J. B., Watson, S. W., Guillard, R. R. L., Brand, L. E. 1979. Widespread
712 occurrence of planktonic cyanobacterium, *Synechococcus*. Nature. 277:293–294

713

714 Yin, Y., Zhang, Y., Wang, M., Shi, K. 2016. Effects of temperature on the optical
715 properties of *Microcystis aeruginosa* and *Scenedesmus obliquus*. J. Freshwater Ecol.
716 31:361–375

717

718 Young, J. N., Goldman, J. A. L., Kranz, S. A., Tortell, P. D., Morel, F. M. M. 2015. Slow
719 carboxylation of Rubisco constrains the rate of carbon fixation during Antarctic
720 phytoplankton blooms. New Phytol. 205:172–181

721

722 Yvon-Durocher, G., Dossena, M., Trimmer, M., Woodward, G., Allen, A. P. 2015.
723 Temperature and the biogeography of algal stoichiometry. Glob. Ecol. Biogeogr. 24:562–
724 570

725

Tables

Table 1. Slope (-E_a, eV) of the ordinary-least-squares linear regression between 1/KT and the natural logarithm of carbon-specific photosynthesis (P^C) and respiration (R^C) for both nutrient treatments, N-limited and N-replete, and growth rate (μ) of the N-replete treatment. 95 % confidence intervals (CI) are given for each estimate.

Variable	Treatment	-*Ea*	n	95% CI	*p*
P^C	N-limited	-0.02	7	-0.62, 0.59	0.95
P^C	N-replete	-0.32	4	-1.43, 0.79	0.35
R^C	N-limited	0.11	7	-0.23, 0.44	0.45
R^C	N-replete	-1.6	4	-3.92, 0.72	0.10
μ	N-replete	-0.49	4	-0.76, -0.21	0.02

Figure legends

Fig. 1 Relationship between temperature and the abundance, expressed as percentage of total protein content, of a) both subunits of RuBisCO and b) PSII core reaction center protein D1, PsbA, for each nutrient supply treatment. Nutrient supply conditions ranged from nutrient-limited growth in continuous cultures at two dilution rates (0.1 d^{-1} and 0.3 d^{-1}) to nutrient-replete growth in semi-continuous batch cultures (N-replete).

Fig. 2 Relationship between the abundance of PsbA and RuBisCO, expressed as a percentage of total protein content, under each nutrient treatment (represented by symbols). The four data points for each nutrient treatment correspond to the four assayed temperatures (represented by colours in a grey scale).

Fig. 3 Relationship between temperature and in situ RbcL abundance a) relative to total protein and b) relative to chlorophyll *a* (note Y-axis in logarithmic scale), in samples from three cruises spanning polar, temperate and tropical latitudes (64˚N to 78˚S). Data are binned and averaged every 5°C and bars indicate standard errors. $R^2 = 0.83$, n = 7, $p < 0.01$ and $R^2 = 0.42$, n = 7, $p = 0.12$ for the linear regression between temperature and RbcL:Total Protein or RbcL:Chl*a*, respectively.

Fig. 4 Relationship between temperature and a) carbon to nitrogen ratio (C:N) and b) carbon to chlorophyll *a* ratio (C:Chl*a*) for the three nutrient supply treatments. Bars indicate standard deviation. Data for N-limited cultures taken from Marañón et al. (2018).

755 Fig. 5 Temperature dependence of a) C-specific CO_2 fixation (P^C), b) Chlorophyll *a*-
756 specific CO_2 fixation ($P^{Chl\,a}$), c) C-specific respiration rate (R^C) under nutrient-limited
757 continuous growth at two different dilution rates (0.1 and 0.3 d^{-1}) and nutrient-replete,
758 exponential growth, and d) growth rate (μ) under nutrient replete conditions. Bars indicate
759 standard deviation. Data for N-limited cultures taken from Marañón et al. (2018).

760

761 Fig. 6 Arrhenius plots for a) Carbon-specific photosynthesis (P^C, h^{-1}) and b) Respiration
762 (R^C, h^{-1}) under N-limited and N-replete conditions and c) growth rate (μ, d^{-1}) under N-
763 replete conditions.

764 Fig. 1

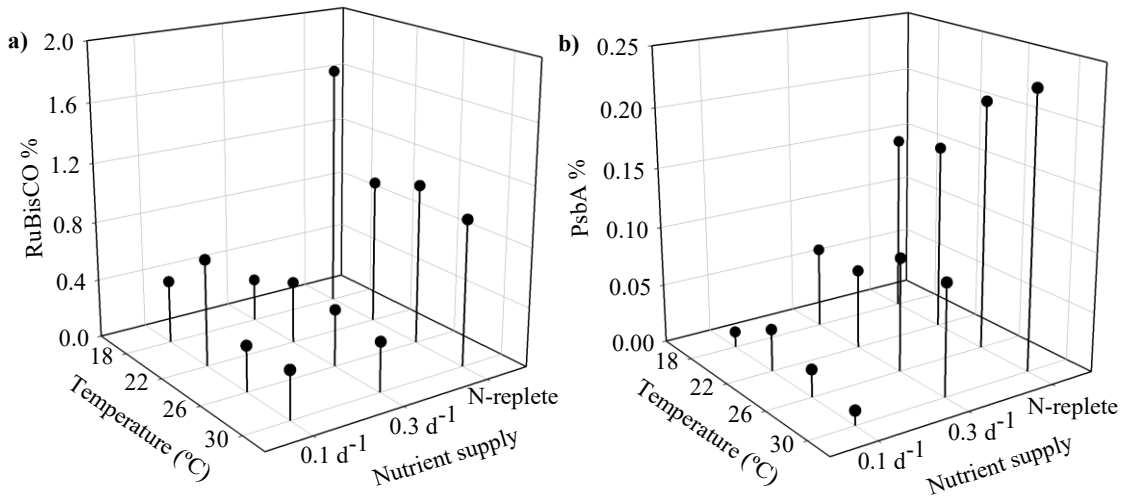

765

766

767 Fig. 2

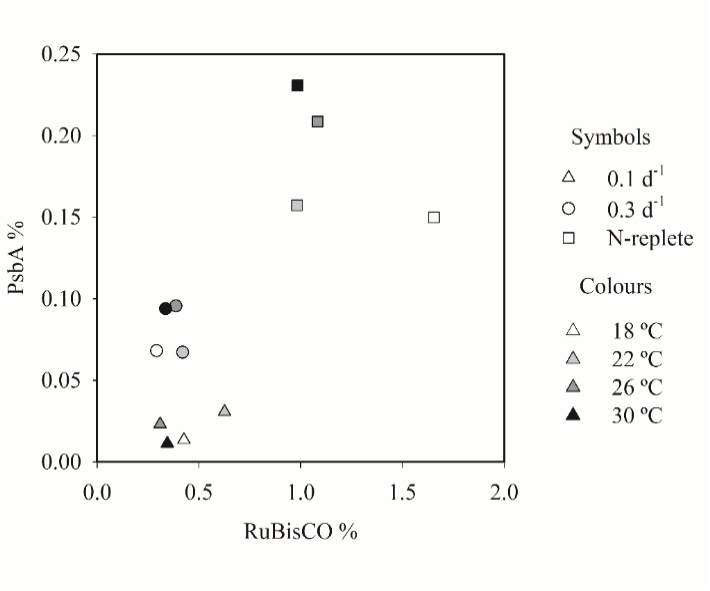

768

769

770 Fig. 3

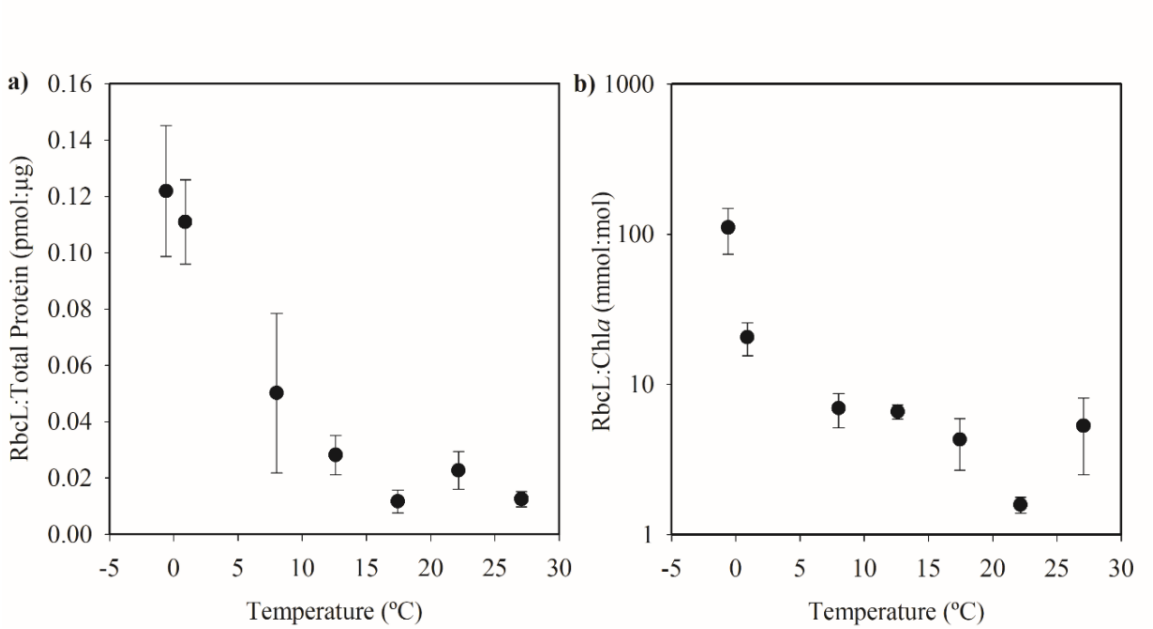

771

772

773 Fig. 4

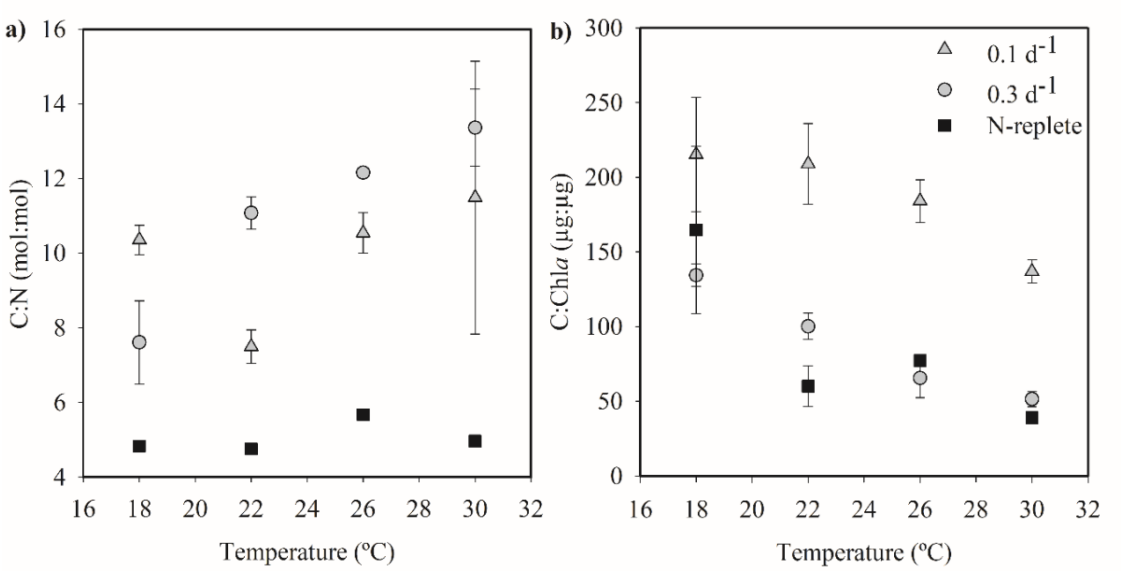

774

775

776 Fig. 5

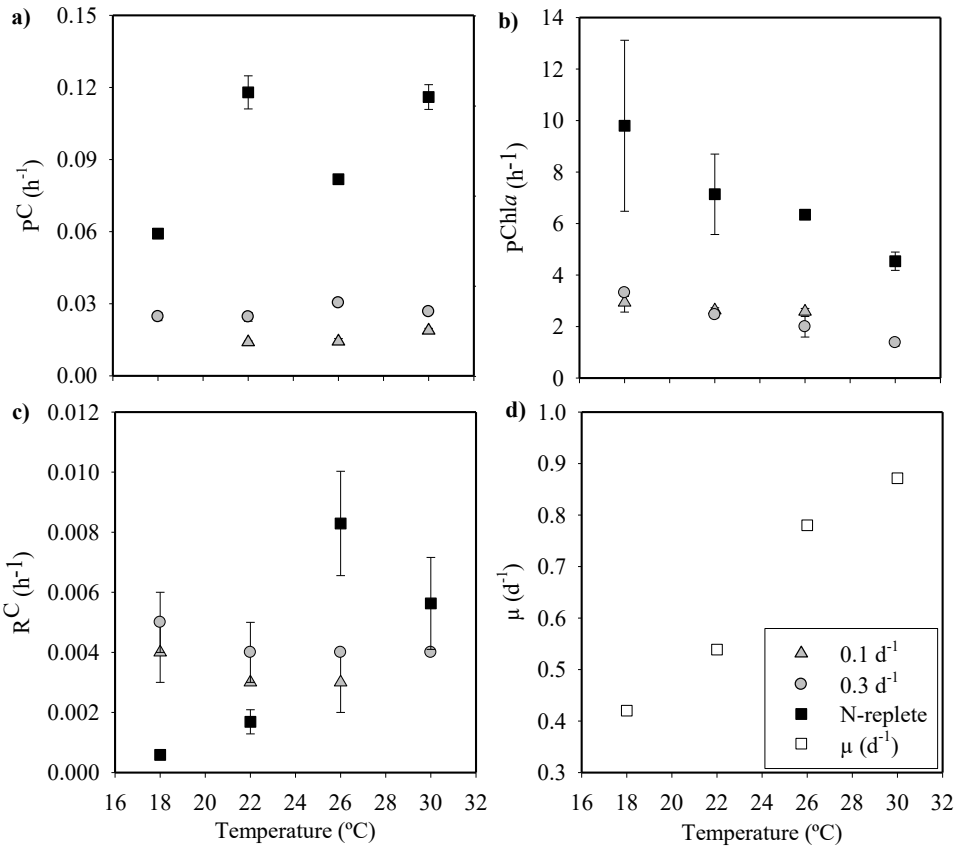

777

778

779 Fig. 6

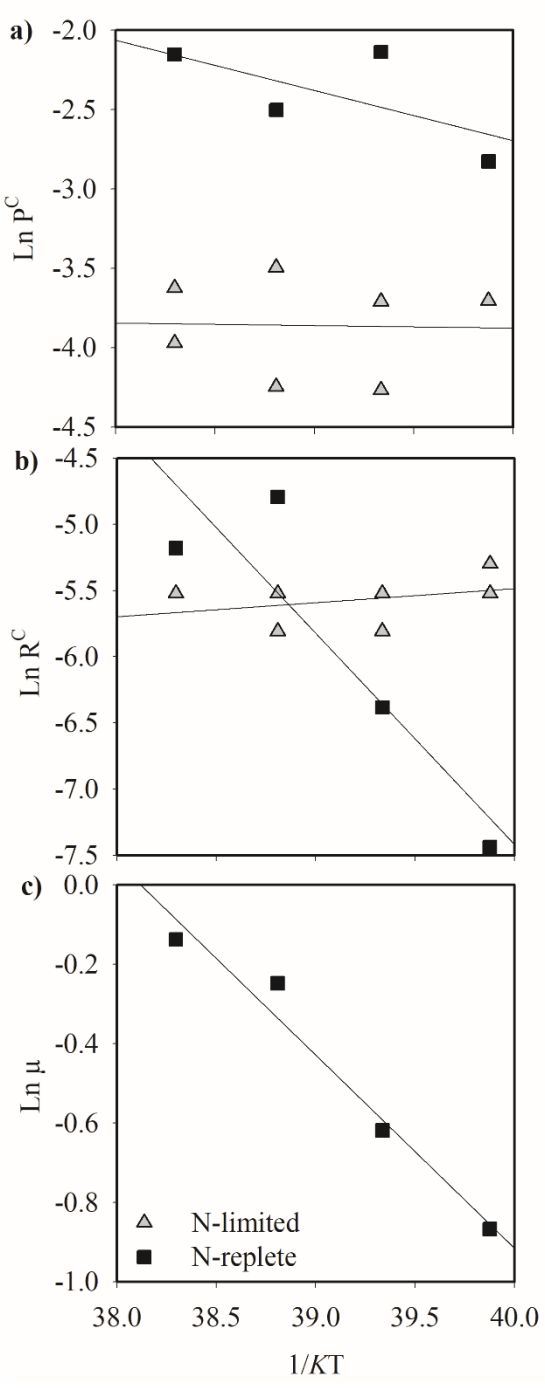

780

781

Supporting information

Article title: EFFECTS OF TEMPERATURE AND NUTRIENT SUPPLY ON RESOURCE ALLOCATION, PHOTOSYNTHETIC STRATEGY AND METABOLIC RATES OF *SYNECHOCOCCUS* SP

Authors: Cristina Fernández-González, María Pérez-Lorenzo, Nicola Pratt, C. Mark Moore, Thomas S. Bibby and Emilio Marañón

The following Supporting Information is available for this article:

Fig. S1 Relationship between temperature and normalized PsbA abundance

Fig. S2 Relationship between temperature and the PsbA to RbcL abundance ratio for each nutrient supply treatment

Fig. S3 Relationship between temperature and the RbcL:Chla and PsbA:Chl*a* ratios for each nutrient supply treatment

Table S1 Abundance of RbcL and PsbA for each experimental treatment

Table S2 Linear regression analyses with temperature and growth rate as independent variables and protein abundance, cellular composition and metabolic rate as dependent variables

Fig. S1 Relationship between temperature and normalized PsbA abundance for the 0.3 d^{-1} nitrogen-limited and nutrient-replete (N-replete) treatments. Normalisation was conducted by dividing PsbA abundance by the mean abundance in each nutrient treatment, so that the effect of nutrient supply was removed. Line represents the linear regression relationship (R^2 = 0.84, n = 8, p = 0.001).

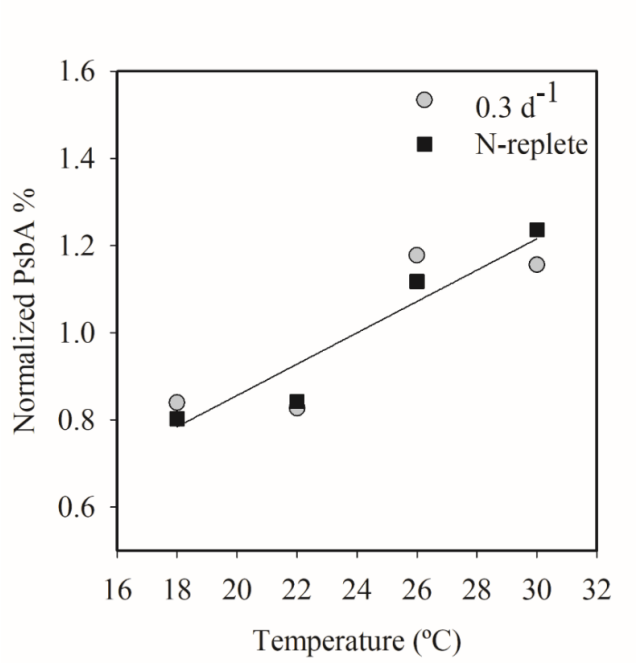

Fig. S2 PsbA to RbcL abundance ratio as a function of temperature for each nutrient nutrient supply treatment. Bars represent standard deviations.

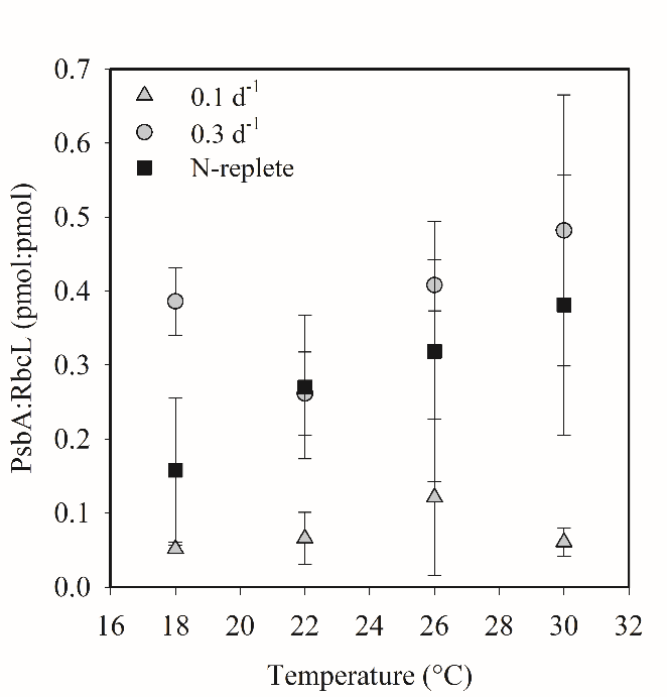

Fig. S3 Relationship between temperature and the abundance (relative to chlorophyll *a* content) of a) RuBisCO large subunit, RbcL, and b) PSII core reaction center protein D1, PsbA, for each nutrient supply treatment. Nutrient supply conditions ranged from nutrient-limited growth in continuous cultures at two dilution rates (0.1 d^{-1} and 0.3 d^{-1}) to nutrient-replete growth in semi-continuous batch cultures (N-replete).

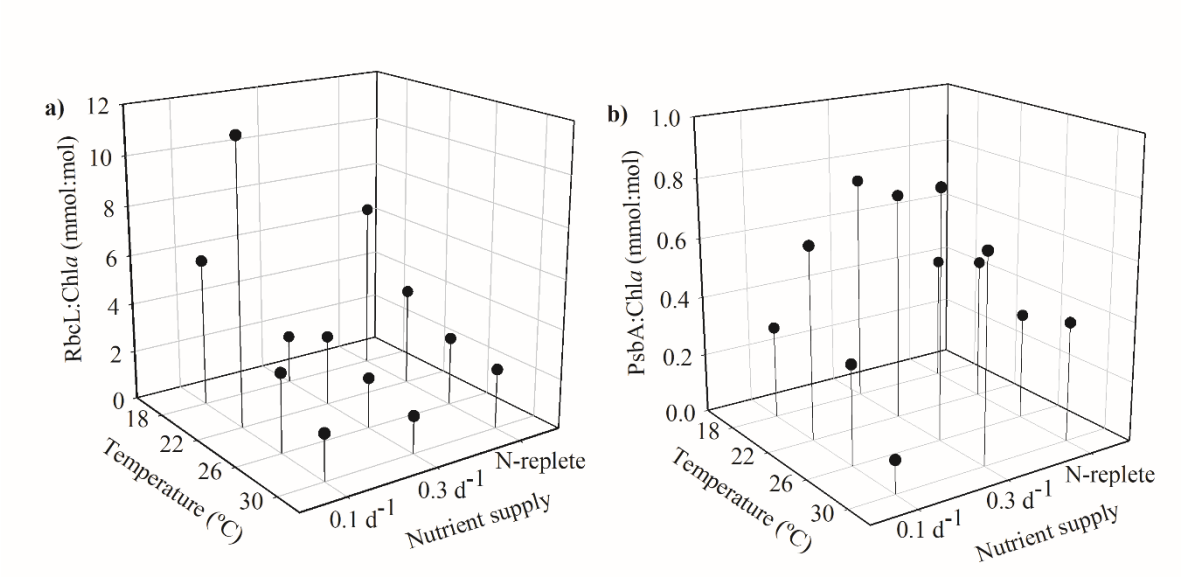

Table S1. Abundance of RbcL and PsbA (pmol) standardized by the content of total protein · (µg of total protein) and by the chlorophyll a content (pmol Chla) for each experimental treatment. Mean (n = 2 and n = 4 for the N-limited and N-replete treatments, respectively) and standard deviation values are given.

µ (d-1)	Temperature (°C)	pmol RbcL (µg Total Protein)$^{-1}$	SD	pmol PsbA (µg Total Protein)$^{-1}$	SD	mmol RbcL (mol Chl*a*)$^{-1}$	SD	mmol PsbA (mol Chl*a*)$^{-1}$	SD
0.1	18	0.065	0.006	0.003	0.001	5.97	1.68	0.31	1.2
0.1	22	0.110	0.026	0.008	0.006	11.47	6.1	0.65	0.0
0.1	26	0.047	0.002	0.006	0.005	3.20	0.99	0.34	2.2
0.1	30	0.050	0.019	0.003	0.000	1.87	0.26	0.11	0.2
0.3	18	0.045	0.003	0.017	0.001	1.98	0.32	0.76	0.3
0.3	22	0.064	0.003	0.017	0.004	2.85	0.4	0.76	2.7
0.3	26	0.059	0.004	0.024	0.000	2.05	0.21	0.83	0.1
0.3	30	0.051	0.013	0.024	0.003	1.52	0.41	0.69	0.8
0.42	18	0.253	0.068	0.038	0.020	6.75	2.91	0.42	1.8
0.54	22	0.150	0.030	0.040	0.013	3.95	1.04	0.48	1.8
0.78	26	0.166	0.030	0.053	0.030	2.79	1.2	0.36	1.3
0.87	30	0.151	0.022	0.058	0.031	2.41	0.58	0.40	1.5